Equilibrium and Transport for Quasi Helical Reversed Field Pinches

S. Cappello 1), D. Bonfiglio1), D.F. Escande 2), S.C. Guo 1), I. Predebon 1), F. Sattin 1), M. Veranda 1), P. Zanca 1), C. Angioni 3), L. Chacon 4), J.Q. Dong 5), X. Garbet 6), S.F. Liu 7)

1) Consorzio RFX – Associazione EURATOM-ENEA sulla fusione – Padova, Italy

2) Laboratoire PIIM, UMR 6633 CNRS-Aix Marseille Université, France

3) Max Planck Institut für Plasmaphysik, EURATOM Association, Garching, Germany

4) Oak Ridge National Laboratory, Oak Ridge, Tennesse, USA

5) Institute for Fusion Theory and Simulation, Zhejiang University, Hangzhou; Southwestern Institute of Physics, Chengdu, People's Republic of China

6) CEA, IRFM, F-13108 Saint Paul Lez Durance, France

7) Department of Physics, Nankai University, Tianjin 300071, People's Republic of China

E-mail contact of main author: susanna.cappello@igi.cnr.it

Abstract. We provide a survey of the recent progresses in theoretical/numerical studies on the physics of the quasi helical RFP regime. Such regime systematically characterizes RFX-mod experiments at high currents (Ip>1.2 MA), producing clear electron transport barriers about mid-radius. Several approaches, ranging from macroscopic to microscopic description, have been used to tackle the related complex physics. MHD analytical calculation of ohmic helical states by perturbation theory has been developed. A necessary criterion for field reversal at the edge is derived, proved to be satisfied in a large database of RFX-mod pulses. Numerical simulations show that the criterion works for large perturbations of the pinch configuration too, in particular those leading to states with a single helical axis. The addition of heat transport dynamics is expected to improve the 3D nonlinear MHD modelling of RFP self-organization. To this end the PIXIE3D initial value code has been implemented for RFP dynamics. Recently, for the first time in MHD simulation, the mandatory step of numerical verification has been completed by careful benchmarking PXIE3D and SpeCyl codes. The effect of chaos healing by separatrix expulsion, believed to favor the formation of transport barriers, has been reviewed using a volume preserving field line tracing code (NEMATO). The nature of additional physical mechanisms responsible for the actual transport in such regimes is matter of study. ITG microturbulence has been considered first. In 2008 Guo showed analytically that ITG modes are more stable in RFPs than in tokamaks because of a stronger Landau damping. In the last two years different numerical tools have been adapted to the RFP: the nonlinear gyrokinetic GS2 code and the fluid TRB code. An integral eigenvalue approach, retaining finite Larmor radius effects has also been used. All approaches agree that ITG modes can hardly become linearly unstable but could be envisaged in future higher-current experiments. Impurities and trapped electrons effect on ITGs are under consideration, first results show a destabilizing effect by impurities, while a negligible one by trapped electrons. Trapped Electron Modes may appear across high density gradient regions. Microtearing turbulence is expected to play an important role at the transport barriers.

1. Introduction

In the Reversed Field Pinch (RFP) RFX-mod experiment, increasing plasma current (Ip>1.2 MA) allows entering progressively better self-organized quasi helical regimes: in such regimes (named Single Helical Axis, SHAX) magnetic chaos reduction is diagnosed together with the formation of clear electron transport barriers [1,2,3]. A similar tendency to access quasi helical regimes, at least from the point of view of magnetic features, is also clearly observed in MST experiment, especially at high current (Ip≈0.5MA) with shallow reversal conditions [4]. We present here developments in theoretical understanding and modeling tools adopted to deal with the RFP helical regime, in particular: advancements in MHD modeling (equilibrium and 3D nonlinear dynamics), and first results concerning the possible impact of electrostatic and electromagnetic turbulence.

2. Macroscopic Description of Reversed Field Pinch Helical Regimes

The theory of helical states in the RFP has been developed essentially on the basis of MHD simulations. Nonlinear 3D visco-resistive modelling of cylindrical RFPs has highlighted since the early 90ties the occurrence of a dynamical bifurcation mainly ruled by the product (viscosity x resistivity) [see Ref. 5 and references therein]. In fact, after passing through intermediate quasi-helical regimes, fully 3D turbulent dynamics turns into laminar 2D helical RFP states (corresponding to stable ohmic equilibria), whenever the other effects (like dissipation) hamper nonlinear coupling between the MHD modes. Those studies also predicted the topological features typical of Quasi Single Helicity (QSH) regimes, namely the development of the chaos-resilient Single Helical Axis (SHAx) states, by separatrix expulsion from the Double Axis (DAx) states (with large magnetic island); thus, they anticipated the experimental observation of similar quasi helical regimes. Altogether, MHD modelling provided confidence in a positive trend, which can actually be recognised in experiments so far, toward stable helical RFP, closer to the theoretical chaos-free Single Helical ohmic states. To progress from previous studies, the development of an ohmic equilibrium solver for helical RFP and the implementation of additional physics in 3D nonlinear dynamics are in our priorities, first results in these directions are described in the following.

2.1. Single Helicity Ohmic Equilibrium

Recent progress in the analytical calculation of ohmic single helicity (SH) states for the RFP has been achieved. This calculation is performed in the frame of resistive MHD in cylindrical geometry, by using perturbation theory for a paramagnetic pinch with low edge conductivity and axial magnetic field. A necessary criterion for the toroidal field reversal at the edge is derived. The criterion involves the radial profile of the logarithmic derivative of the Newcomb eigenfunction of the pinch. It is suggestive that a finite edge radial magnetic field might be favorable for field reversal. In accordance with this, visco-resistive MHD simulations show that helical equilibria with low perturbation amplitudes achieve reversal when a finite edge radial magnetic field is applied. Numerical simulations show that the criterion works for large perturbations of the pinch too, in particular those leading to states with a single helical axis. The necessary criterion is found to be satisfied in the RFX-mod experiment for reversed states with non zero reference edge radial magnetic field. These experimental and numerical results show that the validity of the criterion is more general than suggested by the perturbative approach used for its derivation: nonlinear corrections look weak, and condition $T_{e,edge} \ll T_{e,center}$ sounds as a leading factor. The dynamo velocity field is analytically computed as a result of the ohmic equilibrium equations. In fact, the dynamo velocity which has been mysterious for long in the RFP, finds its drive by a helical electrostatic potential and its origin in the current density modulation along helical magnetic field lines [6]. From this point of view a SH ohmic state turns out to be similar to a saturated tearing mode. Interestingly, the MHD dynamo velocity itself intrinsically features a maximum in the shear profile, which occurs at the location of the safety factor maxima, which in turn is located nearby the foot of experimental transport barriers [7]. This provides an indication of a likely mutual interaction between MHD aspects and possible microturbulence effects.

2.2. Nonlinear 3D MHD Simulation

The nonlinear 3D MHD codes SpeCyl and PIXIE3D have been carefully benchmarked in their common limit of application (visco-resistive MHD in a cylinder) [8]. Nonlinear dynamics for (2D) Tokamak-like and (both 2D and 3D) RFP configurations are "correctly"

predicted by the two codes, providing a first successful example of nonlinear 3D verification benchmark of MHD codes. To show the excellent agreement between the two codes in both linear and nonlinear phases, the temporal evolution of magnetic energy for MHD modes is plotted in Fig.1 for different 2D and 3D simulation cases. The capability of the fully implicit PIXIE3D code to work with time steps comparable with the Alfvén time without loss of accuracy is also shown.
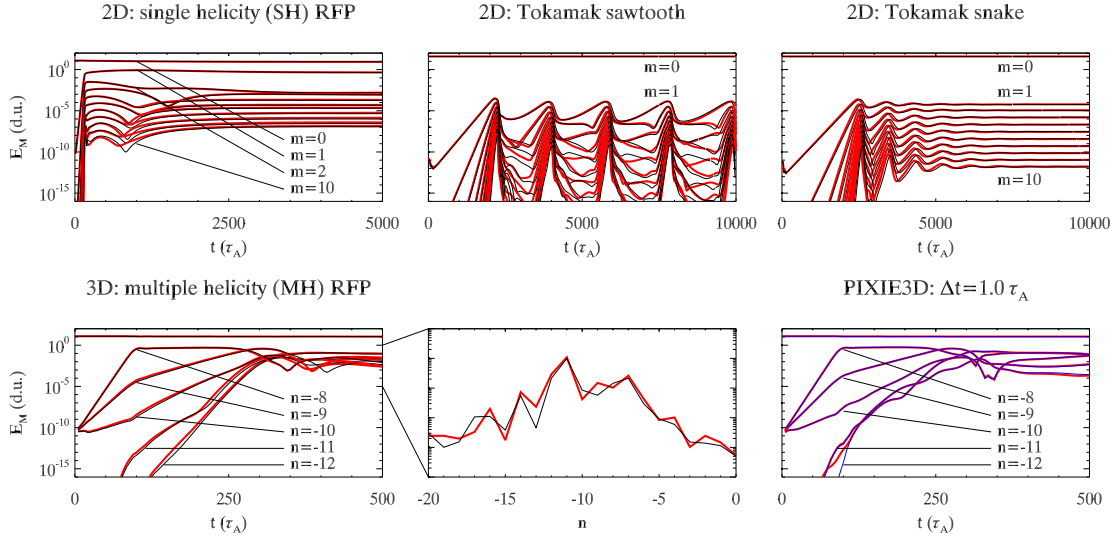

FIG. 1. Nonlinear verification benchmark: Magnetic energy evolution from SpeCyl and PIXIE3D (black and red curves respectively). Top panels) RFP and Tokamak 2D dynamics. Bottom left) 3D RFP case. Bottom right) PIXIE3D with different time steps (red $\Delta t=5x10-3\ \tau_A$ and blue $\Delta t=1\ \tau_A$)

Numerical studies of finite beta and toroidal geometry effects in the RFP with PIXIE3D are now ongoing. Together with this MHD tool, the field line tracing code NEMATO [9] for magnetic topology studies has also been benchmarked against the magnetic flux surfaces computed from a 2D magnetic field (with either helical or poloidal symmetry) provided by MHD simulations.
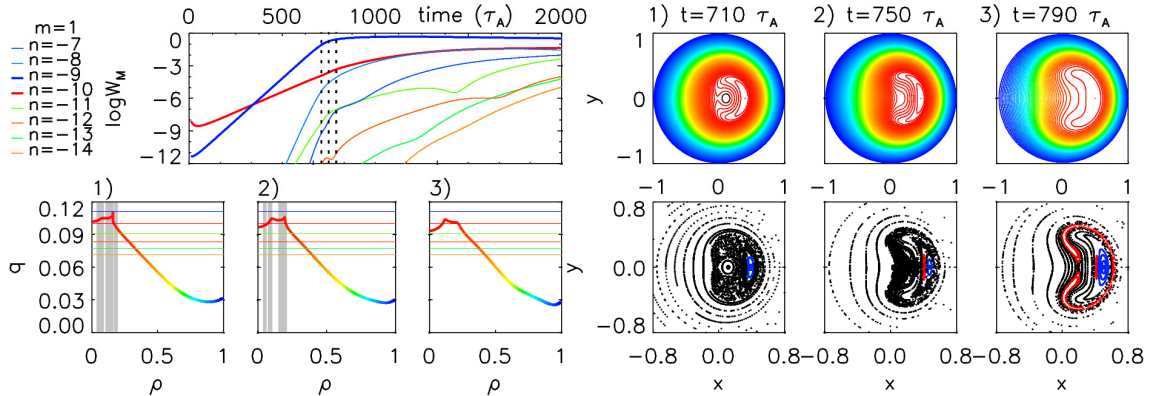

FIG. 2. Chaos healing effect at a transition to quasi-helical SHAx state along a SpeCyl simulation. . Temporal evolution of the magnetic energy of m=1 modes (top left panel). For three chosen times are shown: helical flux surfaces (top right) and helical q-profile (bottom left) given by the dominant n=-9 mode (being ρ the flux function label), Poincaré plots (bottom right) by the code NEMATO.

This volume preserving tool is suitable to deal with 3D cases characterized by weak chaos, like in the RFP. In Fig.2. we show a first application on a SpeCyl simulation case featuring a transition to a SHAx regime: the chaos healing effect after the expulsion of the magnetic separatrix of the dominant mode's island, highlighted in previous works [10], has been clearly

confirmed. In DAx stage a maximum in the helical q profile indicates the position of the dominant mode island separatrix. While mode amplitudes increase the magnetic chaos by secondary modes spreads inside the dominant island. A secondary reversal of the magnetic shear occurs rather soon in DAx stage. Minor conserved structures start to appear at the location of suach secondary q-maxima (local healing of the chaos previously generated). Finally, after expulsion of the dominant mode separatrix -SHAx stage- chaos is definitely removed, despite further growth of secondary modes.

3. Transport in low magnetic chaos RFP: microturbulence studies

As recalled above, the effect of chaos healing by separatrix expulsion (transition to SHAx state) was predicted by previous theoretical/numerical modeling [10]. More recently it has been experimentally diagnosed that in SHAx states strong electron transport barrier isolate a hot helical core (Te up to 1.5 eV) extending in some cases over more than a half of the plasma diameter [7]. In such regimes electron temperature and density become helical flux functions to a good approximation [1]. RFP transport appears therefore no longer dominated by magnetic chaos, yet larger than present neoclassical estimates [11]. The issue, then, remains concerning the nature of additional physical mechanisms determining the resulting confinement in such regimes. Given previous indications of a possible role of Ion Temperature Gradient (ITG) turbulence in producing anomalous momentum transport (viscosity) [5,12], ITG microturbulence has been considered first. In 2008 Guo showed analytically that ITG modes are more stable in RFPs than in Tokamaks because of a stronger Landau damping due to the shorter magnetic field connection length [13]. In the last two years different numerical tools originally developed for tokamak turbulence studies have been adapted to the RFP: the nonlinear electromagnetic (flux-tube) gyrokinetic code GS2 [14,15,16] and the full-radius fluid (electrostatic) code TRB incorporating Landau damping via a Hammet-Perkins closure term [17,18]. In addition, an integral eigenvalue approach, retaining full Finite-Larmor-Radius effects (derived from the linear gyrokinetic equation in electrostatic limit) has also been used to further confirm and extend previous linear results [19]. The main modifications needed to deal with the RFP geometry are related to the large poloidal component of the magnetic field (i.e. low safety factor): hence curvature and grad B drifts enter the equations within a different ordering than in a tokamak.
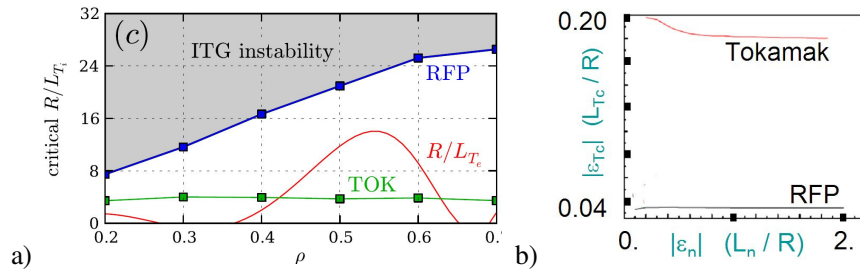

Fig.3. Comparison of ITG threshold values between RFP and Tokamak.
a) GS2 results: threshold (critical R/L_{Ti}) as a function of the normalized plasma radius $\rho=r/a$. (typical RFP (blue line) and Tokamak (TOK green line) cases; Experimental estimate for R/L_{Te} profile in RFP case (red curve). b) Integral eigenvalue approach results: ITG stability threshold is shown as a function of the density gradient ($\varepsilon_n=L_n/R$) for RFP (black) and Tokamak (red).

All approaches agree that, neglecting impurities effects, ITG modes hardly become linearly unstable in present experimental conditions. Due to a lack of direct measurement of ion temperature gradients, such studies have been carried out considering them in the range of 0.5÷1.0 times the electron ones. Marginal stability conditions are reached locally in QSH states with the steepest temperature gradients, or in the plasma edge. Given the experimental

trends, ITG instabilities could thus become a concern in future higher-current experiments. Landau damping is confirmed to be the most important vehicle to damp ITG turbulence in the RFP. At mid-radius the normalized logarithmic temperature gradient R/L_{Ti} has typically to exceed a threshold more than 5 times larger than in a tokamak with the same geometry to trigger instability (Fig.3.).

Present analyses include: i) studies on the effect of impurities and non-adiabatic electrons on ITG instabilities; ii) occurrence of Trapped Electron Modes (TEM); iii) first (fluid) nonlinear simulations of ITG turbulence; iv) linear investigations on electromagnetic instabilities. In the following sections most recent advancements are described.

3.1. Ion Temperature Gradient modes: Impact of impurities

RFX-mod plasmas are ordinarily polluted by carbon and oxygen impurities, yielding Zeff ≥ 2 throughout most of the radius. This raises the question whether impurities may play a role in destabilizing ITGs. First indications from linear stability analysis have been obtained by solving the gyrokinetic integral eigenmode equation, for conditions typical of present experiments (Nz/Ne ~ 2% , with Nz total impurity particle number, where CIII to CVI are the main impurity species, Ne total electrons). Impurities are found to destabilize ITG modes at the locations where a specific relationship occurs between electrons and impurities gradients: $L_{eZ} = L_n/L_Z < 0$ (L_n and L_z are the density gradient scale length of the hydrogen and z component of the impurity respectively). In RFX-mod plasma, and especially in SHAx states, the impurities (mainly carbon ions) tend not to accumulate in the core, instead they remain mostly distributed nearby the plasma edge, around the region of r > 0.6a [20]. For this peculiar feature, where the electron density profile normally decreases, the carbon ions, having peaked profiles in the same region, possess a positive slope; hence the condition $L_{eZ} <$ 0 is easily verified. In fact, the computation by integral eigenmode equation shows that in the r>0.6a region ITG mode can be unstable. The Impurity Driven Mode [21] may also become unstable for conditions observed in some recent RFX-mod shots. The destabilizing effect by impurities on ITG modes in the RFP can be understood as follows: the thermal velocity of impurities is smaller than that of the main ions due to their larger mass, therefore Landau damping is less important for the impurities. In addition, the density gradient of the main ions becomes steeper where L_{eZ} increases, which leads to increase the frequency of ITG mode. This also decreases the impact of the ion Landau damping for the main ions. Minor changes are expected from heavier impurities.

3.2. Trapped Electron Effects on ITG and Trapped Electron Modes (TEM)

In the RFP plasma the fraction, f, of trapped particles reaches almost the same values as in the tokamak (where f ~ $(2\varepsilon)^{1/2}$, with ε =r/R). The difference is that in the RFP case magnetic mirroring results from both the poloidal and toroidal components of the field. The resulting trapped particle fraction is lower than in the tokamak mainly in the edge, and is f ~ $(2\delta)^{1/2}$ [22], where $\delta < \varepsilon$ across the whole radius, δ taking explicitly into account B_θ and the finite plasma beta.

In the ITG mode study, the trapped-electron effect has not significant influence on the mode behavior. This is expected since the mode propagates in the ion diamagnetic drift direction and no resonance is found in the trapped-electron response. The strong ion Landau damping is still the dominant effect. This has been verified analytically, and also using both GS2 and TRB by artificially turning off the trapped electron fraction. A slightly destabilizing effect is found, but the critical temperature gradients are essentially unaltered. As an example, in Fig.4.a the effect of the inclusion of trapped electrons is shown for a GS2 simulation.

Conversely, preliminary indications show that Trapped Electron Modes (TEM) instabilities can arise in the presence of strong enough density gradients. In the limit $R/L_n \gg 1$, GS2 simulations show that TEMs are the dominant electrostatic instability at work at the ion Larmor radius scale. This result is also confirmed analytically, by solving the differential eigenmode equation (Fig.4.b). However, RFX-mod plasmas are usually characterized by flat core density profiles. TEM turbulence is therefore expected to potentially play a role in the edge of the RFP plasma.
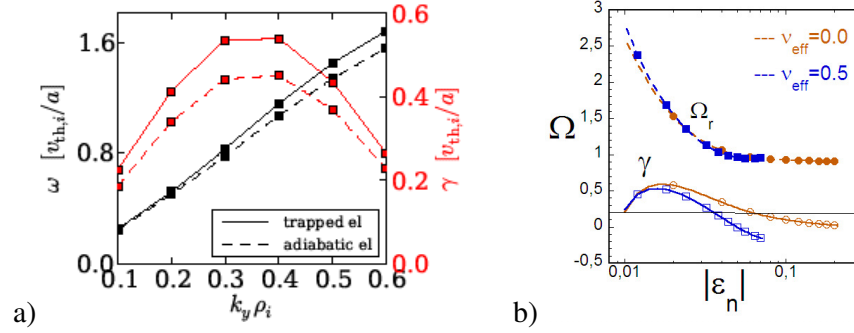

FIG. 4. a) Effect of trapped electrons on real frequency and growth rate spectra of ITG modes (solid lines) with respect to the case with adiabatic electrons (dashed lines).
b) TEM in RFP plasmas: growth rate, γ, and the frequency, Ω_r, for peaked electron temperature profiles ($\varepsilon_{Te}=L_{Te}/R= -0.025, \eta_e=0.4\text{-}8$) and flat ion temperature profiles ($\eta_i \approx 0$). $k_\theta \rho_i =0.447$. $\varepsilon_n=L_n/R$; $\nu_{eff} = \nu_{ei}/\delta$. All frequencies are normalized by ($v_{thi}/Rq\alpha$). Only fluid ions are considered.

3.3. Nonlinear time-dependent TRB simulations of ITG turbulence

Being a global code, TRB allows for studying possible synergies between different turbulence drives, spatially extended and not necessarily localized at the same position. As a first step in this direction, we started studying the relaxation of an initial linearly-ITG-unstable temperature profile under the action of the self-consistent ITG-driven conductivity (χ_{NL}), with the addition of a spatially shaped constant-in-time background conductivity (χ_{back}). Consistently with indications from some experimental cases in which magnetic chaos appear to persist in the outer plasma regions, in this first simple test case, χ_{back} has been assigned a sharply increasing radial profile, of the order of the collisional value in the core, and larger by more than one of order of magnitude in the outer half radius. In this simulation the ratio T_i/T_e is held fixed at unity value. The heat source is kept uniform and constant throughout the whole radius (a rather simplistic schematization for RFPs, where the heating is purely ohmic). The q profile is held fixed (monotonically decreasing) too. A sensitivity study with respect to all of these key ingredients is going to be performed in the next future. The nonlinear relaxation of an initially unstable temperature profile is shown in Fig.5.
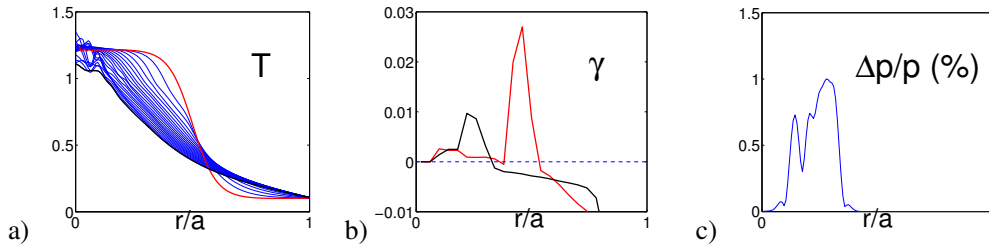

Fig. 5. a) Ion temperature profile (initially strongly ITG-unstable, red curve) evolves (blue curves) under self-generated turbulent transport. The final profile (black) is close to the asymptotical one. b) Maximum growth rates for initial and final temperature profiles: large positive initial values (red) evolve toward marginal conditions (black). c) Radial spread of ITG turbulence at final stage.

As seen in Fig.5., the location of maximum growth rate shifts from about the mid-radius (red curve) to smaller radii, as long as the threshold condition for instability is satisfied for milder and milder slopes.

3.4. Electromagnetic studies.

GS2 linear simulations have been performed including fluctuations in the magnetic vector potential. The occurrence of microtearing instability has been revealed at the electron temperature barriers of RFX-mod. Indeed, the Microtearing Mode (MT) is a drift-tearing mode destabilized by electron temperature gradients. The growth of MT's may lead to chains of overlapping magnetic islands and subsequent local stochastization of magnetic field lines near mode rational surfaces. Hence MTs may provide an effective contribution to the thermal diffusivity through electron parallel motion along stochastic field lines, which in the past has been considered to play a role in Tokamaks [see e.g. 23]. However, since it was argued that these modes become stable when electron collision frequency decreases substantially below the electron diamagnetic frequency, and since most present-days tokamaks are effectively collisionless in the core, the study of MTs was relegated to the edge region. More recently, interest in these modes was revived in connection with Tokamak ITBs, where large temperature gradients are sustained (see, e.g., [24]). RFX-mod features presently a moderate peak temperature ($1 \div 1.5$ keV) which, coupled to the strong internal temperature gradients, should represent an optimal environment for these modes to grow. The GS2 analysis presented here is based on typical profiles of experimental SHAx, where the collision frequency, ν, and the electron diamagnetic frequency, $\omega*$, stay around $\nu \approx 10\ \omega*$. The dominant instability turns out to be of MT type (Fig.6.), the tearing nature is revealed by the parity of the mode, the sign of the frequency and the strong localization of the parallel magnetic vector potential. MTs thus represent a potential contribution to turbulent transport at the location of the ITB, where R/L_T is maximum.
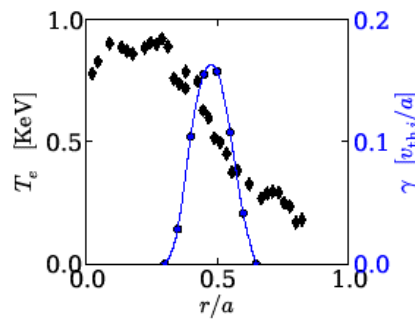

Fig.6. Electron temperature profile (diamonds), and growth rate of the most unstable MT modes (solid curve with circles).

An estimate of the related heat conductivity can be derived in terms of the quasi-linear expression: $\chi \approx b^2\ u_{th,e}\ L_{corr}$. Inside this expression, the only quantity known accurately is the electron thermal speed $u_{th,e}$. The normalized amplitude of magnetic field perturbations is estimated according to the quasilinear criterion by Drake *et al* [23]: $b \approx \rho_e /L_T$, ρ_e being the electron Larmor radius. Concerning the longitudinal correlation length L_{corr}, it was verified by using the field-line-tracing code NEMATO [9] that $L_{corr} \approx 2\pi a$. The conductivity is thus estimated: $\chi \approx 5 \div 20$ m^2/s. This figure is fairly compatible with experimental power-balance estimates at the ITB that yield $\chi \approx 5 \div 50$ m^2/s [7]. This supports the view that a relevant fraction of the turbulent transport across the ITB can be driven by MTs.

4. Summary, final remarks and perspectives

In the last years, the RFP configuration at high plasma currents has been observed to naturally access a self-organized quasi-helical regime characterized by a strong reduction of magnetic chaos. A promising "bifurcation" in confinement properties is seen, and the plasma complexity common to other confinement configurations, revealed for example by the occurrence of transport barriers, calls for new efforts in theoretical-numerical modeling. Besides of further improving the macroscopic description, as obtained by MHD numerical modeling traditionally developed for the RFP, the possible impact of microturbulence has been tackled with a set of tools adapted from the Tokamak environment. Within MHD, a necessary criterion for magnetic field reversal provides a first step toward analytical calculation of helical ohmic equilibria. A recent successful verification benchmark of 3D nonlinear MHD codes (SpeCyl & PIXIE3D), including the application of NEMATO code for topology diagnosis has been completed. Microturbulence studies by different approaches (gyrokinetic and gyrofluid) provide first results: an intrinsic robustness of the RFP to ITG instability is indicated, even if a possible threat comes from the tendency of RFP impurities to accumulate in the edge. The general indication is that ITG activity might become a concern in next future, given the present experimental trends in strengthening the transport barriers of QSH regimes. Microtearing turbulence, instead, is indicated as a likely player in present experimental conditions. The interplay between the MHD scale and transport effects, like the impact of microturbulence, remains a challenging common objective for fusion application.

References
[1] Lorenzini R., et al., Nature Phys. **5**, 570 (2009).
[2] Cappello S., et al., AIP Conf. Proc. **27** 1069 (2008).
[3] Puiatti M.E., et al., Plasma Phys. Control. Fusion **51** 124031 (2009).
[4] Franz P., et al., APS-DPP Conference, Chicago, USA (2010)
[5] Cappello S., Plas. Phys. Contr. Fus. **46** B313 (2004).
[6] Bonfiglio D., et al., Phys. Rev. Lett. **94** 145001 (2005).
[7] Puiatti M. E., et al., this conference: IAEA-FEC Daejeon, Korea, EX-M1, (2010)
[8] Bonfiglio D., et al., Phys. Plasmas **17**, 082501 (2010).
[9] Finn J.M. and Chacon L., Phys. Plasmas **12** 054503 (2005).
[10] Escande D. F., et al., Phys. Rev. Lett. **85** (2000).
[11] Marrelli L., et al., this conference: IAEA-FEC Daejeon, Korea, EX/P5-10, (2010)
[12] Terranova D. et al. Plas. Phys. Contr. Fus. **42**   n. 7   843 (2000).
[13] Guo S.C., Physics of Plasmas **15** 122510 (2008).
[14] Kotschenreuther M., et al., Comp. Phys. Comm. **88** 128 (1995)
[15] Dorland W., et al., Phys. Rev. Lett. **85**, 5579 (2000).
[16] Predebon I., et al., Phys. Plasmas **17** 012304 (2010).
[17] Garbet X and Waltz R E Phys. Plasmas **3** 1898 (1996)
[18] Sattin F., et al., Plasma Phys. Control. Fusion XXXX (2010)
[19] Liu S. F., et al., Phys. Plasmas **17**, 052505 (2010)
[20] Menmuir S., et al., Plasma Phys. Control. Fusion **52** 095001 (2010)
[21] Dong J.Q. and Horton W., Phys. Plasmas **2** 3412 (1995)
[22] Gobbin M. et al., J. Plasma Fusion Res. Series **8** 1147 (2009)
[23] Drake J.F., et al., Phys. Rev. Lett. **44** 994 (1980)
[24] Horton W., ``Microtearing and ETG Modes'', workshop ``Multi-scale Interaction between magnetic islands and micro-turbulence in magnetic fusion devices'', Aix-en-Provence, France (2010), http://sites.univ-provence.fr/~lia-fjmfl/workshop2010/Horton1.pdf.